Electrochemical H2 Production using Polypyrazole based Zinc(II) Complex in Alkaline Medium

Mohamed Ibrahim, Gaber A.M. Mersal, Ahmed Fallatah, Rabah Boukherroub, Safaa Abdou, Mohammed Amin

Asian Journal of Chemistry; Vol. 34, No. 6 (2022), 1366-1372

ASIAN JOURNAL OF CHEMISTRY

https://doi.org/10.14233/ajchem.2022.23669

Electrochemical H_2 Production using Polypyrazole based Zinc(II) Complex in Alkaline Medium

MOHAMED M. IBRAHIM[1,*], GABER A.M. MERSAL[1], AHMED M. FALLATAH[1], RABAH BOUKHERROUB[2], SAFAA N. ABDOU[3] and MOHAMMED A. AMIN[1,*]

[1]Department of Chemistry, College of Science, Taif University, P.O. Box 11099, Taif 21944, Saudi Arabia
[2]Univ. Lille, CNRS, Centrale Lille, Université Polytechnique Hauts-de-France, UMR 8520-IEMN, F 59000 Lille, France
[3]Chemistry Department, Khourma University College, University of Taif, Taif, Saudi Arabia

*Corresponding author: E-mail: ibrahim@tu.edu.sa

Received: 6 November 2021; *Accepted*: 22 December 2021; *Published online*: 18 May 2022; AJC-20794

A zinc(II) complex of polypyazole containing ligand namely, [Tp*ZnCl] (**Zn1**) {Tp* = *tris*(3,5-dimethylpyrazolyl)borate}, along with its zinc(II) bound hydroxo complex [Tp*Zn–OH] (**Zn2**) were synthesized and characterized by FT-IR, Raman, ^{1}H NMR techniques and elemental analysis. In alkaline solution (0.1 M KOH), the **Zn2** modified glassy carbon (GC), namely GC–**Zn2**, was investigated as a molecular electrocatalyst for the hydrogen evolution reaction (HER). Different quantities (*ca.* 0.1–0.5 mg cm^{-2}) of **Zn2** were loaded on GC electrodes to make various GC–**Zn2** electrodes. These electrodes were utilized as cathodes in 0.1 M KOH to produce H_2 using linear sweep voltammetry (LSV) measurements. The HER electrocatalytic activity of the GC–**Zn2** catalyst was found to be quite high and it increased with the catalyst loading density. The top performing electrocatalyst, GC–**Zn2** (0.5 mg cm^{-2}), demonstrated considerable HER catalytic performance with a low HER onset potential (E_{HER}) of –33 mV *vs.* RHE and a high exchange current density of 0.59 mA cm^{-2}. Moreover, the top performing electrocatalyst had a Tafel slope of –152 mV dec^{-1} and consumed an overpotential of 135 mV to generate a current density of 10 mA cm^{-2}. Under the same operating conditions, these HER electrochemical kinetic parameters were found to be not remarkably far from those determined for commercial Pt/C (–10 mV *vs.* RHE, 0.88 mA cm^{-2}, 108 mV dec^{-1} and 110 mV to yield a current density of 10 mA cm^{-2}). In addition, the most active molecular electro-catalysts for H_2 production from aqueous alkaline electrolytes were found to be comparable to the HER electrochemical kinetic parameters reported here for the GC–**Zn2** electrocatalyst. Using 5000 cycles of repetitive cyclic voltammetry and 48 h of chronoamperometry measurements, the best electrocatalyst's stability and long term durability were tested. It exhibited high stability for the HER catalytic activity.

Keywords: Tripod ligand, Zinc(II) complex, Molecular electrocatalyst, Hydrogen evolution reaction.

INTRODUCTION

Earth's environment has suffered greatly as a result of the world's recent reliance on fossil-fuel-generated electricity. As a result, efforts have been made to address concerns such as (i) lowering CO_2 levels in the atmosphere and (ii) designing and implementing a carbon-free energy system. While alternative energy sources such as wind and solar energy exist, they are constrained by geographic limits and a lack of effective storage mechanisms for the energy produced. The challenge can be solved by developing a non-fouling energy carrier that can be used to store chemical energy [1].

Hydrogen has been proposed as a potential sustainable energy carrier with a variety of uses [1-4]. Designing systems that produce H_2 using electrochemical water splitting is a long term method of converting electrical energy into clean fuel that can be realized in an H_2 economy. The hydrogenase enzymes [5,6] are portrayed as naturally occurring microorganisms that efficiently catalyze the reversible interconversion of protons to hydrogen using earth-abundant metals (Ni and Fe) with high turnover rates (6000-9000 ([Fe–Fe]) and 700 ([Ni-Fe]) moles of H_2 per mole of enzyme per second for the HER [7-9]. Enzymes, on the other hand, are difficult to manufacture in large enough quantities for commercial usage and their stability outside of their native system is often limited [10,11].

The structural and functional mimicking of hydrogenase's active site has recently gotten a lot of attention [12-14]. As a result, the development of highly efficient, stable and robust

HER molecular electrocatalysts for the creation of hydrogen, which are inexpensive and made of earth abundant transition metal elements and different ligand combinations, has piqued interest in the community [15-41].

The present work's target is to synthesize and fully characterize a Tp^*–based zinc(II) complex [Tp^*ZnCl] (**Zn1**) {Tp^*= *Tris*(3,5-dimethylpyrazolyl)borate), along with zinc(II) bound hydroxo complex, Tp^*Zn–OH. It was also the purpose of the present work is to investigate the synthesized zinc(II) bound hydroxo complex [Tp^{MeMe}Zn(OH)] (**Zn2**) as a molecular electrocatalyst for the HER in an aqueous alkaline solution of KOH (0.1 M) employing LSV technique. Continuous cyclic voltammetry (5,000 cycles) and chronoamperometry techniques (48 h of severe cathodic polarization conditions) were used to test the long term stability and durability of the electrocatalyst (**Zn2**).

EXPERIMENTAL

Ligand hydro*tris*(3,5-dimethylpyrazolyl)borate (KTp^{MeMe}) was synthesized following a published method [42].

Solutions: Chemical reagents of analytical grade (Sigma-Aldrich) were freshly synthesized using Millipore Milli-Q filtered water (resistivity: 18.2 M cm). To begin, 4 mg of **Zn2** was dispersed in a 4:1 ratio (v/v) mixture of deionized water and ethanol to create a homogenous, well-dispersed electrocatalyst ink. The mixture was then mixed with 80 mL of Nafion. After 30 min of sonicating the mixture, the electrocatalyst produces a homogenous ink. A mass load of 0.1 mg cm^{-2} was obtained by dropping 5 mL of this homogeneous ink on a well-polished glass carbon (GC) electrode (3 mm in diameter) and drying it in the air. Two more GC loaded complex **1** electrodes with mass loading densities of 0.3 and 0.5 mg cm^{-2} were made using the same procedure.

Cell and apparatus and electrochemical setup: In deaerated 0.1 M KOH aqueous solutions, the electrocatalytic behaviour of the three GC loaded **Zn2** electrodes towards the HER was examined using a typical jacketed three electrode cell.

RESULTS AND DISCUSSION

Characterization of the ligand and its zinc(II) complex: The synthesis of **Zn1** was performed in absolute methanol by reacting the ligand KTp^{MeMe} with $ZnCl_2$ in 1:1 ratio, which was further deprotonated by using KOH, forming the zinc(II)–bound hydroxo species **Zn2**. The presence of the bulky methyl groups on the pyrazolyl rings are found to be important for the stabilization of the obtained tetrahedral zinc(II) complex. The analytical and spectral results demonstrated that the investigated complexes havae a 1:1 zinc(II):ligand stoichiometry with molar conductance value in the range of 34-39 W cm^2 mol^{-1}, proposing that both Cl^- and OH^- anions are bound to the central zinc(II) ion in solution (**Scheme-I**).

IR and Raman spectra: The IR data showed that the free ligand exhibits bands at 1627 and 692 cm^{-1}, attributed to the ν(C=N) and δ(pyazole ring), respectively. The pyrazole ring breathing is traced at 972 cm^{-1}. Upon complexation, the bands due to δ(pyrazole ring) observed an upward shift by about 4-18 cm^{-1}. These indicated that the coordination of the three pyrazolyl nitrogens N_3 has been taken place (**Scheme-I**). This mode of binding to zinc(II) ion is further confirmed by the observation of new absorption band at 435-420 cm^{-1}, which is not shown in the spectrum of the free ligand, which is assignable to ν(Zn–N) [43,44]. The B–H stretch (2436 cm^{-1}) in the free ligand KTp^* shifted to higher energies 2509 and 2512 cm^{-1} for **Zn1** and **Zn2**, respectively. In the OH stretching region in complex **Zn2** (Fig. 1), a very broad absorption band appeared in 3350-3320 cm^{-1}, which is identified for the coordinated hydroxide anion [45].

^{1}H NMR spectra: The zinc(II) bound hydroxo complex species **Zn2**, will be used as electrocatalyst the alkaline medium was obtained by the reaction of **Zn1** with an equimolar amount of KOH in absolute methanol. Fig. 2 shows the ^{1}H NMR spectra of **Zn1** and its deprotonating hydroxo complex **Zn2** in DMSO–d_6. The ^{1}H NMR spectrum of **Zn2** exhibits reson-ances at 2.27 (9H, singlet), 2.41 ppm (9H, singlet), 5.74 (3H, singlet), which are assigned to the methyl and pyrazolyl protons. The positions of these proton signals were shifted compared to those found in **Zn1**, indicating the formation of the hydroxo species.

Electrochemical characterizations for the HER: The LSV curves for the GC–**Zn2** electrodes with varying loading densities (*ca.* 0.1-0.5 mg cm^{-2}) are shown in Fig. 3a. The experiments were carried out in a deaerated aqueous solution of KOH (0.1 M) at room temperature. At a potential scan rate of 5.0 mV s^{-1}, the working electrode's potential is cathodically polarized from the corresponding corrosion potential to a cathodic potential value of –1.0 V *vs.* RHE. All currents were referred to the electrochemical active surface area (EASA)

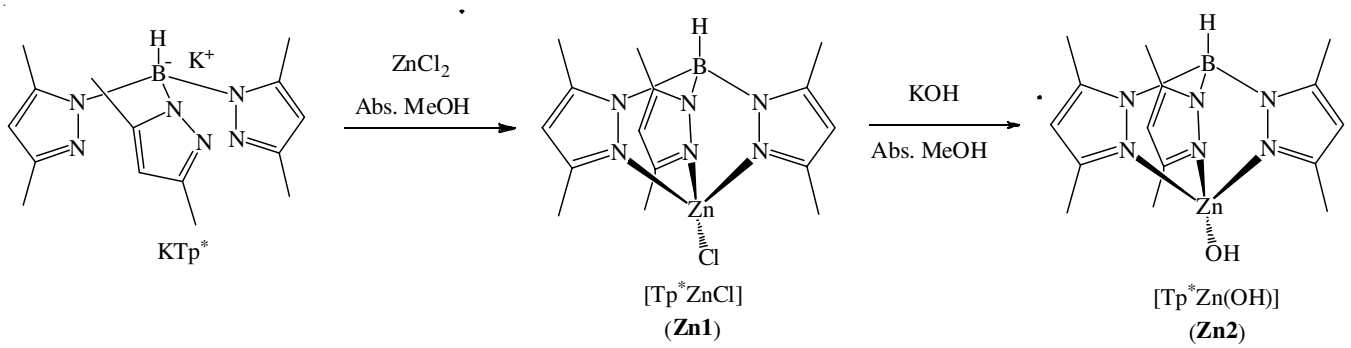

Scheme-I: Structures of zinc(II) complexes **Zn1** and **Zn2**

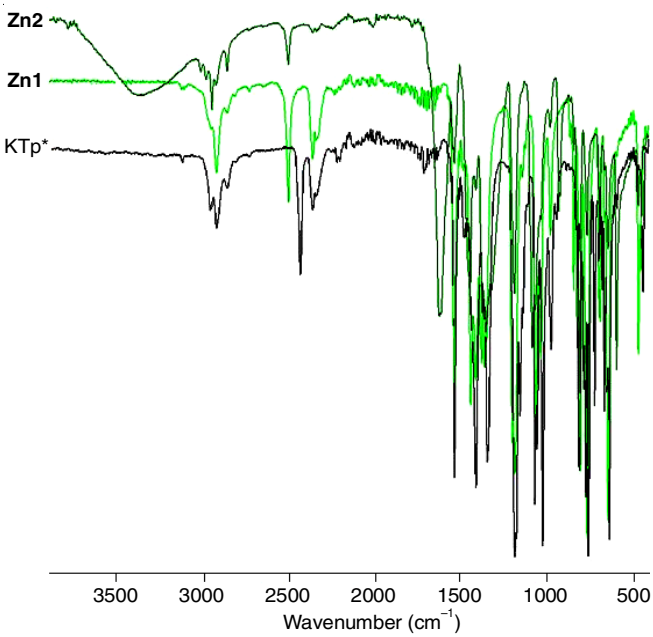

Fig. 1. FT-IR spectra of the ligand KTp* and its zinc(II) complexes **Zn1** and **Zn2**

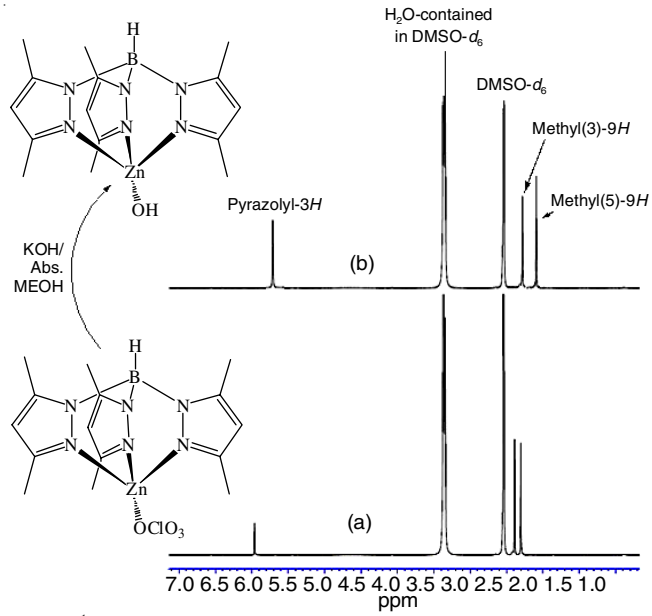

Fig. 2. ^{1}H NMR spectra of zinc(II) complexes **Zn1** and its hydroxo complex **Zn2**

determined from the impedance measurements carried out at different overpotentials, see later.

Fig. 3b shows the Tafel plots derived from the LSV's data, Fig. 3a. Such plots were constructed to gain more insight into the electrocatalytic behaviour of the examined catalysts. Table-1 shows the electrochemical kinetic characteristics of the HER obtained from Tafel plots.

The HER's onet potential (E_{HER}) value, the potential at which the reduction of H_2O molecules is commenced to generate H_2 and beyond which the gas is abundantly evolved corresponding to increased cathodic current (*i.e.* enhanced HER catalytic activity), is used to evaluate and compare the examined catalysts' HER electrocatalytic performance.

Because any change in its placement on the polarization curve causes a significant change in the numerical value of j_o, which affects HER catalytic activity, this potential is considered a critical electrochemical kinetic property that measures the catalyst's HER catalytic performance. Because it creates large quantities of H_2 with higher j_o values at low overpotentials, an electrocatalyst with a low E_{HER} value is described as an efficient HER electrocatalyst in the literature [46-51].

The three examined GC–**Zn2** electrodes (curves 2–4) demonstrated considerable current gains at lower E_{HER} values as compared to the GC electrode (curve 1), which decreased further as the **Zn2** loading density increased, moving towards the anodic (active) direction. This suggests that as the loading density of **Zn2** increases, hydrogen generation is favoured at

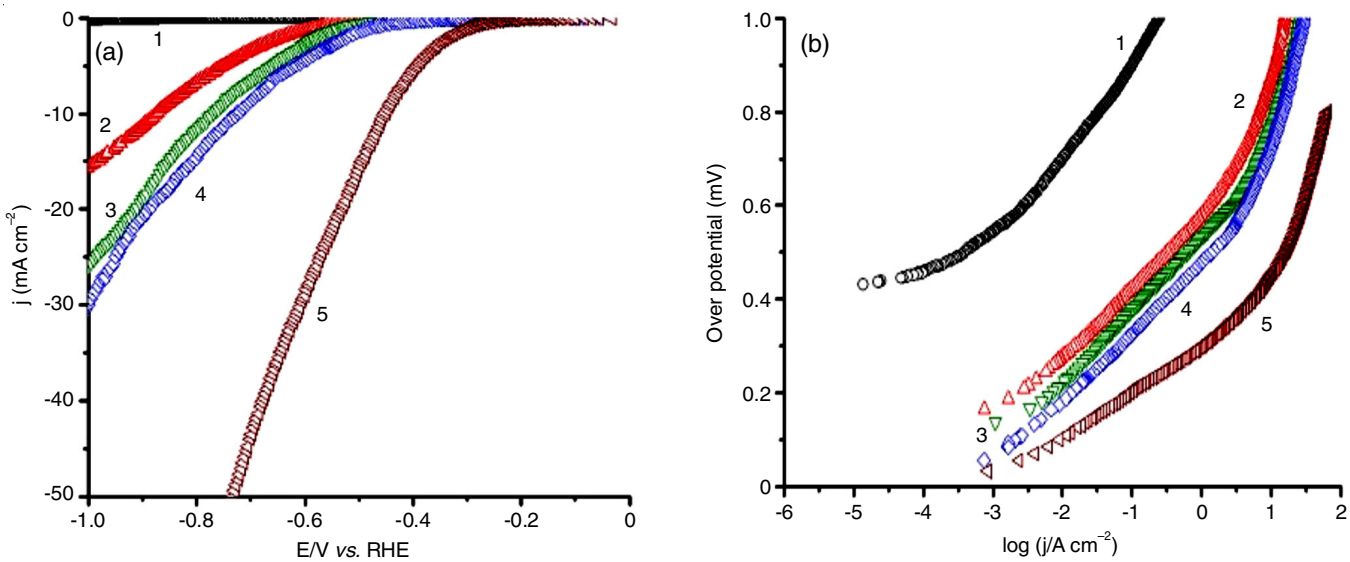

Fig. 3. (a) LSV measurements constructed for the studied **Zn2** of various loading densities in a comparison with bare GC and Pt/C. Measurements were carried out in 0.1 M KOH aqueous solution at a scan rate of 5.0 mV s^{-1} at room temperature. (b) Tafel plots derived from the LSV data (a). (1) bare GC; (2) GC-**Zn2** (0.1 mg cm^{-2}); (3) GC-**Zn2** (0.3 mg cm^{-2}); (4) GC-**Zn2** (0.5 mg cm^{-2}); (5) Pt/C

TABLE-1
HYDROGEN EVOLUTION REACTION (HER) ELECTROCHEMICAL KINETIC PARAMETERS' MEAN VALUE (STANDARD DEVIATION) CALCULATED FOR THE TESTED CATALYSTS

Tested cathode	E_{HER} (mV) (RHE)	$-\beta_c$ (mV dec^{-1})	j_o (mA cm^{-2})	η_{10} (mV)
Bare GC electrode	–	254 (6.0)	$6.3\ (0.15) \times 10^{-4}$	–
GC-**Zn2** (0.1 mg cm^{-2})	115 (2.3)	155 (3.1)	$16.9\ (0.32) \times 10^{-2}$	240 (4.3)
GC-**Zn2** (0.3 mg cm^{-2})	65 (1.5)	157 (2.6)	$35.4\ (0.8) \times 10^{-2}$	186 (3.2)
GC-**Zn2** (0.5 mg cm^{-2})	33 (0.8)	152 (2.3)	$58.8\ (1.1) \times 10^{-2}$	135 (2.4)
Pt/C	10 (0.2)	113 (1.2)	$88\ (1.2) \times 10^{-2}$	110 (1.4)

low overpotential levels, resulting in better HER kinetics. These data show that increasing **Zn2** loading density boosts the HER in a catalytic way.

The overpotential value (η_{10}) acquired by an electrocatalyst to generate a current density value of 10 mA cm^{-2} is an important electrochemical kinetic metric to compare and analyze the catalytic performance of electrocatalysts [52]. Table-1 shows that, similar to E_{HER}, the value of η_{10} decreases as the catalyst loading density increases. When the electrocatalyst loading density is raised, the efficient synthesis of hydrogen at lower overpotentials is confirmed. These results confirm the effectual generation of hydrogen at reduced overpotentials when the electrocatalyst loading density is raised.

The exchange current density (j_o) value increased significantly as the loading density of **Zn2** increased, indicating increased catalytic activity. This is evident from the j_o values shown in Table-1, which range from 0.17 mA cm^{-2} for a loading density of 0.1 mg cm^{-2} to 0.35 and 0.59 mA cm^{-2} for loading density values of 0.3 and 0.5 mg cm^{-2}, respectively. Based on its HER electrochemical kinetic parameters, namely E_{HER}, j_o, β_c and η_{10}) the GC–**Zn2** (0.5 mg cm^{-2}) electrocatalyst outperformed most active HER molecular electrocatalysts described in the literature, as shown in Table-1.

Tafel slope is a well-known HER electrochemical kinetic parameter for comparing and evaluating the performance of electrocatalysts. It can also be utilized to determine the rate determining step and forecast the HER reaction pathway. The Tafel slope, in practice, shows the overpotential increment required to generate a ten-fold increase in current density. As a result, a small Tafel slope value indicates a rapid increase in electrocatalytic current density at lower overpotential values, implying increased catalytic activity [53].

Parallel Tafel lines can be clearly seen for all three GC–**Zn2** catalysts examined, with Tafel slopes ranging from 152 to 157 mV dec^{-1}. These findings suggest that the loading density of the complex under consideration has no influence on the Tafel slope value. The catalyst layer therefore causes an unappreciated internal resistance, according to these studies [54]. The high Tafel slopes imply that the Volmer-Heyrovsky reaction, with the Volmer step as the rate determining step, governs the HER kinetics [55-58].

The electrochemical active surface area (EASA), which is directly related to the HER kinetics HER on the electrocatalysts' surfaces, is another significant measure for comparing the catalytic performance of different electrocatalysts. EASA is also intimately related to the double layer capacitance (C_{dl}) [59-61]. As a result, C_{dl} is utilized to determine the value of EASA. The catalyst's C_{dl} value was calculated using CV measurements performed for each tested catalyst in the non-faradic area as a function of the potential scan rate (about 20-120 mV s^{-1}), see Fig. 4 as an example conducted at a potential sweep rate of 100 mV s^{-1}.

The values of C_{dl} were determined from the slopes of the current density against the potential scan rate plots, Fig. 4b.

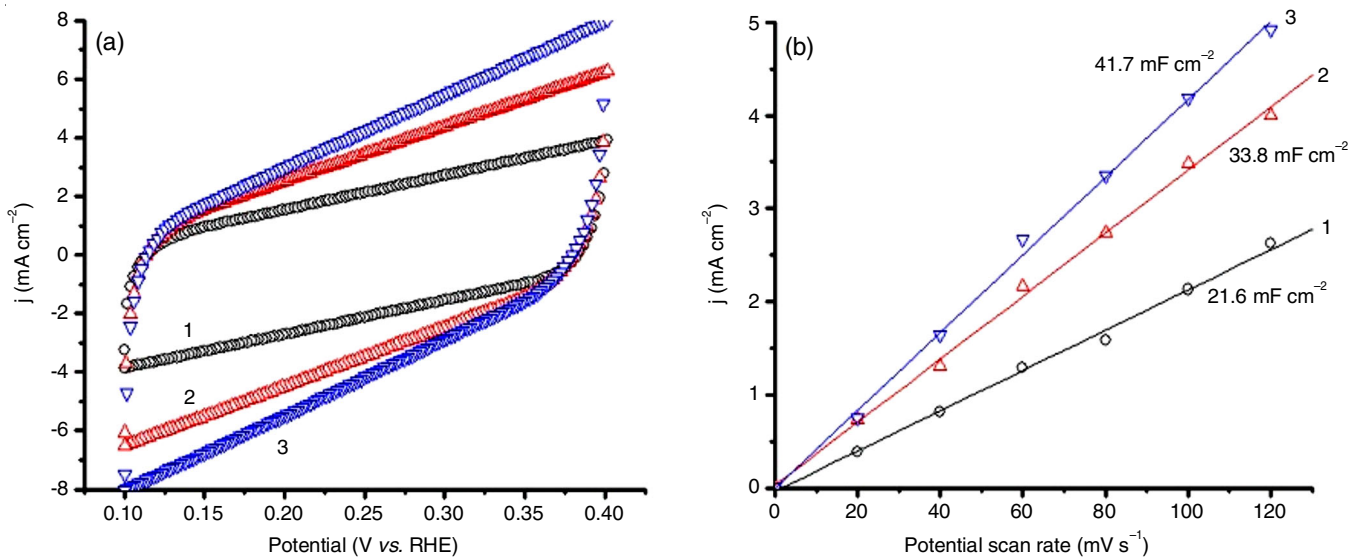

Fig. 4. (a) CV measurements constructed for the studied **Zn2** of various loading densities. Measurements were carried out in 0.1 M KOH aqueous solution at a scan rate of 100 mV s^{-1} at room temperature. (b) Double-layer capacitance measurements for determining the catalyst's electrochemically-active surface area. (1) GC–**Zn2** (0.1 mg cm^{-2}); (2) GC– **Zn2** (0.3 mg cm^{-2}); (3) GC–**Zn2** (0.5 mg cm^{-2})

C_{dl} values of 21.6, 33.8 and 41.7 mF cm^{-2} were respectively estimated for the electrocatalysts GC–**Zn2** (0.1 mg cm^{-2}), GC–**Zn2** (0.3 mg cm^{-2}) and GC–**Zn2** (0.5 mg cm^{-2}). Because electrocatalysts with higher C_{dl} values have a slew more attackable active surface sites, these results confirm the catalytic influence with increasing **Zn2** loading density [59-61]. As a result, efficient charge transfer is accelerated, resulting in improved catalytic efficiency.

The flat electrode's specific capacitance, symbolized here as C_s, with a geometric surface area of (1.0 cm^2), is typically reported in the literature covering a range 20-40 μF cm^{-2}, giving a C_s value of 30 μF cm^{-2} on average [62]. Table-2 shows the EASA values obtained by substituting this average C_s value into eqn. 1 [62].

$$EASA = \frac{C_{dl}}{C_s} \quad (1)$$

Moreover, when the loading density of catalyst increases, the values of EASA also increased (Table-2).

TABLE-2
DOUBLE-LAYER CAPACITANCE (C_{dl}), ELECTROCHEMICAL ACTIVE SURFACE AREA (EASA), NET VOLTAMMETRY CHARGE (Q) AND THE NUMBER OF ACTIVE SITES (n) ESTIMATED FOR THE INVESTIGATED ELECTROCATALYSTS FROM CV MEASUREMENTS

Tested cathode	C_{dl} (mF cm^{-2})	EASA (cm^2)	$Q_{net} \times 10^3$ (C@100 mV s^{-1})	$n \times 10^8$ (mol)
GC–**Zn2** (0.1 mg cm^{-2})	21.6	720	25.86	13.40
GC–**Zn2** (0.3 mg cm^{-2})	33.8	1127	37.94	19.66
GC–**Zn2** (0.5 mg cm^{-2})	41.7	1390	49.52	25.66

Eqn. 2 was used to compute the active sites (n, mol) on the catalyst surface [63]:

$$n = \frac{Q_{net}}{2F} \quad (2)$$

where F stands for the Faraday constant (96485 C/mol) and 2 stands for the number of electrons transported during the HER. The net voltammetry charge (Q_{net}) of the catalyst is computed through subtracting the charges generated by bare GC electrode ($Q_{bare\ GC}$) from the charges produced by the investigated catalyst ($Q_{GC\text{–}}$**Zn2**). The CV data taken at a potential scan rate of 100 mV s^{-1} were used to estimate such Q values (Fig. 4).

The considerable increase in the value of n induced by increasing the loading density of **Zn2** implies increased catalytic activity. The GC–**Zn2** (0.5 mg cm^{-2}) electrocatalyst has the greatest *n* value (25.66 × 10^{-8} per mol) thus, confirming its exceptional HER catalytic activity.

Long-term stability test: The top performing electrocatalyst, GC–**Zn2** (0.5 mg cm^{-2}), was further assessed for stability and long–term durability using CV measurements. Fig. 5 shows the catalyst's first and 5000th cycles. Obviously, the catalyst is particularly stable, as indicated by the humble current loss after completing the 5000th cycle. Tafel slope after the last cycle recorded a value of (156 mV dec^{-1}), which is close to that estimated after the first cycle (152 mV dec^{-1}, Table-1). This finding suggests that catalyst potential cycling has little effect on the HER pathway.

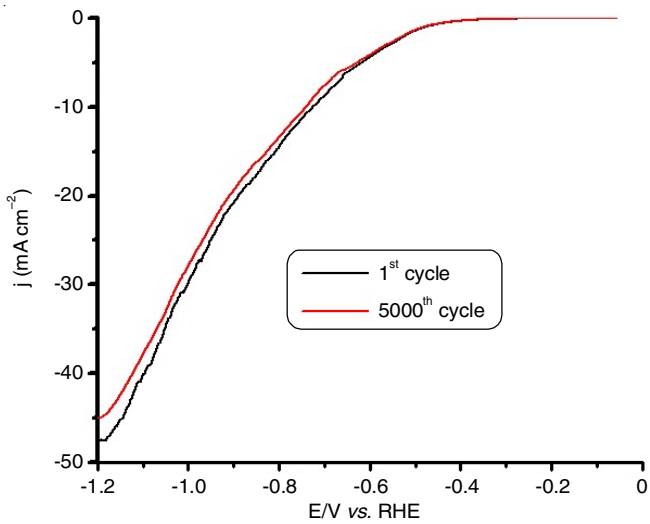

Fig. 5. Long-term stability test recorded for the best performing electrocatalyst, namely GC–**Zn2** (0.5 mg cm^{-2}) in 0.1 M KOH solution at room temperature for the HER. LSV measurements were conducted at a scan rate of 50 mV s^{-1}

Conclusion

A new polypyazoles based zinc(II) complex (**Zn2**) modified glassy carbon (GC) surface was examined as electrocatalysts for the effectual generation of H_2 in 0.1 M KOH. Using the LSV technique, several loading densities (0.1, 0.3 and 0.5 mg cm^{-2}) of GC–**Zn2**, the electrocatalytic activity of the GC–**Zn2** catalyst for the HER was high and it increased as the loading density of the catalyst was increased. The GC–**Zn2** electrocatalyst displayed significant HER catalytic activity with a low onset potential of –33 mV *vs.* RHE and a high exchange current density of 0.59 mA cm^{-2} and a loading density of 0.5 mg cm^{-2}. At a 135 mV overpotential, it also produced a current density of 10 mA cm^{-2}. These electrochemical kinetic parameters were similar to those reported in the literature for the most active molecular electrocatalysts for H_2 production from aqueous alkaline electrolytes. The best electrocatalyst's long term durability was assessed using cyclic voltammetry technique, which was continuously repeated for 5,000 cycles and the results demonstrated its auspicious electrocatalytic stability.

ACKNOWLEDGEMENTS

This study was funded by the Deanship of Scientific Research, Taif University, Saudi Arabia (Project No. 1-439-6070).

CONFLICT OF INTEREST

The authors declare that there is no conflict of interests regarding the publication of this article.

REFERENCES

1. J. Turner, G. Sverdrup, M.K. Mann, P.C. Maness, B. Kroposki, M. Ghirardi, R.J. Evans and D. Blake, *Int. J. Energy Res.*, **32**, 379 (2008); https://doi.org/10.1002/er.1372
2. A. Zuttel, A. Remhof, R. Borgschulte and O. Friedrichs, *Phil. Trans. R. Soc. A*, **368**, 3329 (2010); https://doi.org/10.1098/rsta.2010.0113

3. I. Dincer and C. Acar, *Int. J. Hydrogen Energy*, **43**, 8579 (2018); https://doi.org/10.1016/j.ijhydene.2018.03.120
4. I. Staffell, D. Scamman, A. Velazquez Abad, P. Balcombe, P.E. Dodds, P. Ekins, N. Shah and K.R. Ward, *Energy Environ. Sci.*, **12**, 463 (2019); https://doi.org/10.1039/C8EE01157E
5. K.A. Vincent, A. Parkin and F.A. Armstrong, *Chem. Rev.*, **107**, 4366 (2007); https://doi.org/10.1021/cr050191u
6. J.C. Fontecilla-Camps, A. Volbeda, C. Cavazza and Y. Nicolet, *Chem. Rev.*, **107**, 4273 (2007); https://doi.org/10.1021/cr050195z
7. M.E. Carroll, B.E. Barton, T.B. Rauchfuss and P.J. Carroll, *J. Am. Chem. Soc.*, **134**, 18843 (2012); https://doi.org/10.1021/ja309216v
8. W. Lubitz, H. Ogata, O. Rudiger and E. Reijerse, *Chem. Rev.*, **114**, 4081 (2014); https://doi.org/10.1021/cr4005814
9. C. Tard and C.J. Pickett, *Chem. Rev.*, **109**, 2245 (2009); https://doi.org/10.1021/cr800542q
10. P.M. Vignais and B. Billoud, *Chem. Rev.*, **107**, 4206 (2007); https://doi.org/10.1021/cr050196r
11. T. Goris, A.F. Wait, M. Saggu, J. Fritsch, N. Heidary, M. Stein, I. Zebger, F. Lendzian, F.A. Armstrong, B. Friedrich and O. Lenz, *Nat. Chem. Biol.*, **7**, 310 (2011); https://doi.org/10.1038/nchembio.555
12. M. Gómez-Gallego and M.A. Sierra, *Inorg. Chem. Front.*, **8**, 3934 (2021); https://doi.org/10.1039/D1QI00505G
13. T.R. Simmons, G. Berggren, M. Bacchi, M. Fontecave and V. Artero, *Coord. Chem. Rev.*, **270-271**, 127 (2014); https://doi.org/10.1016/j.ccr.2013.12.018
14. D. Schilter, J.M. Camara, M.T. Huynh, S. Hammes-Schiffer and T.B. Rauchfuss, *Chem. Rev.*, **116**, 8693 (2016); https://doi.org/10.1021/acs.chemrev.6b00180
15. A.M. Abudayyeh, O. Schott, H.L.C. Feltham, G.S. Hanan and S. Brooker, *Inorg. Chem. Front.*, **8**, 1015 (2021); https://doi.org/10.1039/D0QI01247E
16. N. Zaman, T. Noor and N. Iqbal, *RSC Adv.*, **11**, 21904 (2021); https://doi.org/10.1039/D1RA02240G
17. N.K. Oh, J. Seo, S. Lee, H. Kim, U. Kim, J. Lee, Y. Han and H. Park, *Nat. Commun.*, **12**, 4606 (2021); https://doi.org/10.1038/s41467-021-24829-8
18. S. Wang, A. Lu and C. Zhong, *Nano Converg.*, **8**, 4 (2021); https://doi.org/10.1186/s40580-021-00254-x
19. T. Kato, R. Tatematsu, K. Nakao, T. Inomata, T. Ozawa and H. Masuda, *Inorg. Chem.*, **60**, 7670 (2021); https://doi.org/10.1021/acs.inorgchem.0c03657
20. F. Kamatsos, K. Bethanis and C.A. Mitsopoulou, *Catalysts*, **11**, 401 (2021); https://doi.org/10.3390/catal11030401
21. H. Lei, Y. Wang, Q. Zhang and R. Cao, *J. Porphyr. Phthalocyan.*, **24**, 1361 (2020); https://doi.org/10.1142/S1088424620500157
22. Y. Guo, T. Park, J.W. Yi, J. Henzie, J. Kim, Z. Wang, B. Jiang, Y. Bando, Y. Sugahara, J. Tang and Y. Yamauchi, *Adv. Mater.*, **31**, 1807134 (2019); https://doi.org/10.1002/adma.201807134
23. P. Zhang, M. Wang, Y. Yang, T. Yao and L. Sun, *Angew. Chem. Int. Ed.*, **53**, 13803 (2014); https://doi.org/10.1002/anie.201408266
24. H. Lei, H. Fang, Y. Han, W. Lai, X. Fu and R. Cao, *ACS Catal.*, **5**, 5145 (2015); https://doi.org/10.1021/acscatal.5b00666
25. J.-P. Cao, T. Fang, L.-Z. Fu, L.-L. Zhou and S.-Z. Zhan, *Int. J. Hydrogen Energy*, **39**, 13972 (2014); https://doi.org/10.1016/j.ijhydene.2014.07.030
26. L.-Z. Fu, T. Fang, L.-L. Zhou and S.-Z. Zhan, *RSC Adv.*, **4**, 53674 (2014); https://doi.org/10.1039/C4RA07211A
27. J.-P. Cao, T. Fang, Z.-Q. Wang, Y.-W. Ren and S. Zhan, *J. Mol. Catal. Chem.*, **391**, 191 (2014); https://doi.org/10.1016/j.molcata.2014.04.034
28. J. Wang, C. Li, Q. Zhou, W. Wang, Y. Hou, B. Zhang and X. Wang, *Dalton Trans.*, **45**, 5439 (2016); https://doi.org/10.1039/C5DT04628A
29. D.M. Ekanayake, K.M. Kulesa, J. Singh, K.K. Kpogo, S. Mazumder, H. Bernhard Schlegel and C.N. Verani, *Dalton Trans.*, **46**, 16812 (2017); https://doi.org/10.1039/C7DT02711G
30. Z.-J. Xin, S. Liu, C.-B. Li, Y.-J. Lei, D.-X. Xue, X.-W. Gao and H.-Y. Wang, *Int. J. Hydrogen Energy*, **42**, 4202 (2017); https://doi.org/10.1016/j.ijhydene.2016.11.103
31. K. Majee, J. Patel, B. Das and S.K. Padhi, *Dalton Trans.*, **46**, 14869 (2017); https://doi.org/10.1039/C7DT03153J
32. T. Fang, H.-X. Lu, J.-X. Zhao, S.-Z. Zhan and Q.-Y. Lv, *J. Mol. Catal. Chem.*, **396**, 304 (2015); https://doi.org/10.1016/j.molcata.2014.10.008
33. T. Fang, L.-L. Zhou, L.-Z. Fu, S.-Z. Zhan and Q.-Y. Lv, *Polyhedron*, **85**, 355 (2015); https://doi.org/10.1016/j.poly.2014.08.030
34. T. Straistari, R. Hardré, J. Fize, S. Shova, M. Giorgi, M. Réglier, V. Artero and M. Orio, *Chem. Eur. J.*, **24**, 8779 (2018); https://doi.org/10.1002/chem.201801155
35. C.M. Klug, W.G. Dougherty, W.S. Kassel and E.S. Wiedner, *Organometallics*, **38**, 1269 (2019); https://doi.org/10.1021/acs.organomet.8b00548
36. S. Fukuzumi, Y.-M. Lee and W. Nam, *Coord. Chem. Rev.*, **355**, 54 (2018); https://doi.org/10.1016/j.ccr.2017.07.014
37. W.T. Eckenhoff, *Coord. Chem. Rev.*, **373**, 295 (2018); https://doi.org/10.1016/j.ccr.2017.11.002
38. A. Xie, J. Zhu and G.G. Luo, *Int. J. Hydrogen Energy*, **43**, 2772 (2018); https://doi.org/10.1016/j.ijhydene.2017.12.120
39. D. Hong, Y. Tsukakoshi, H. Kotani, T. Ishizuka, K. Ohkubo, Y. Shiota, K. Yoshizawa, S. Fukuzumi and T. Kojima, *Inorg. Chem.*, **57**, 7180 (2018); https://doi.org/10.1021/acs.inorgchem.8b00881
40. J.M. Lei, Q.X. Peng, S.P. Luo, Y. Liu, S.Z. Zhan and C.L. Ni, *Mol. Catal.*, **448**, 10 (2018); https://doi.org/10.1016/j.mcat.2018.01.014
41. G.G. Luo, H.L. Zhang, Y.W. Tao, Q.Y. Wu, D. Tian and Q. Zhang, *Inorg. Chem. Front.*, **6**, 343 (2019); https://doi.org/10.1039/C8QI01220B
42. G. Parkin, *Chem. Rev.*, **104**, 699 (2004); https://doi.org/10.1021/cr0206263
43. J. Perkinson, S. Brodie, K. Yoon, K. Mosny, P.J. Carroll, T.V. Morgan and S.J.N. Burgmayer, *Inorg. Chem.*, **30**, 719 (1991); https://doi.org/10.1021/ic00004a023
44. D.A. Baldwin, A.B.P. Lever and R.V. Parish, *Inorg. Chem.*, **8**, 107 (1969); https://doi.org/10.1021/ic50071a026
45. K. Nakamoto, Infrared Spectra of Inorganic and Coordination Compounds, John Wiley & Sons: New York, p. 256 (1986).
46. M.A. Amin, N. El-Bagoury, M.H.H. Mahmoud, M.M. Hessien, S.S.A. El-Rehim, J. Wysocka and J. Ryl, *RSC Adv.*, **7**, 3635 (2017); https://doi.org/10.1039/C6RA25384A
47. T.N.J.I. Edison, R. Atchudan, N. Karthik and Y.R. Lee, *J. Hydrogen Energy*, **42**, 14390 (2017); https://doi.org/10.1016/j.ijhydene.2017.04.228
48. H. Wang, Y. Cao, G. Zou, Q. Yi, J. Guo, L. Gao, *ACS Appl. Mater. Interfaces*, **9**, 60 (2017); https://doi.org/10.1021/acsami.6b14393
49. M.A. Amin, E.M. Ahmed, N.Y. Mostafa, M.M. Alotibi, G. Darabdhara, M.R. Das, J. Wysocka, J. Ryl and S.S. Abd El-Rehim, J. Ryl and S.S. Abd El-Rehim, *ACS Appl. Mater. Interfaces*, **8**, 23655 (2016); https://doi.org/10.1021/acsami.6b05630
50. M.A. Amin, S.A. Fadlallah, G.S. Alosaimi, F. Kandemirli, M. Saracoglu, S. Szunerits and R. Boukherroub, *Int. J. Hydrogen Energy*, **41**, 6326 (2016); https://doi.org/10.1016/j.ijhydene.2016.02.107
51. G. Darabdhara, M.A. Amin, G.A.M. Mersal, E.M. Ahmed, M.R. Das, M.B. Zakaria, V. Malgras, S.M. Alshehri, Y. Yamauchi, S. Szunerits and R. Boukherroub, *J. Mater. Chem. A Mater. Energy Sustain.*, **3**, 20254 (2015); https://doi.org/10.1039/C5TA05730B
52. J. Tian, Q. Liu, A.M. Asiri and X. Sun, *J. Am. Chem. Soc.*, **136**, 7587 (2014); https://doi.org/10.1021/ja503372r

53. M. Zeng and Y. Li, *J. Mater. Chem. A Mater. Energy Sustain.*, **3**, 14942 (2015); https://doi.org/10.1039/C5TA02974K
54. A.P. Murthy, J. Theerthagiri, J. Madhavan and K. Murugan, *Phys. Chem. Chem. Phys.*, **19**, 1988 (2017); https://doi.org/10.1039/C6CP07416B
55. T. Shinagawa, A.T. Garcia-Esparza and K. Takanabe, *Sci. Rep.*, **5**, 13801 (2015); https://doi.org/10.1038/srep13801
56. J. Durst, A. Siebel, C. Simon, F. Hasché, J. Herranz and H.A. Gasteiger, *Energy Environ. Sci.*, **7**, 2255 (2014); https://doi.org/10.1039/C4EE00440J
57. H. Over, *Chem. Rev.*, **112**, 3356 (2012); https://doi.org/10.1021/cr200247n
58. N.-T. Suen, S.-F. Hung, Q. Quan, N. Zhang, Y.-J. Xu and H.M. Chen, *Chem. Soc. Rev.*, **46**, 337 (2017); https://doi.org/10.1039/C6CS00328A
59. N. Liu, Y. Guo, X. Yang, H. Lin, L. Yang, Z. Shi, Z. Zhong, S. Wang, Y. Tang and Q. Gao, *ACS Appl. Mater. Interfaces*, **7**, 23741 (2015); https://doi.org/10.1021/acsami.5b08103
60. J. Xie, J. Zhang, S. Li, F. Grote, X. Zhang, H. Zhang, R. Wang, Y. Lei, B. Pan and Y. Xie, *J. Am. Chem. Soc.*, **135**, 17881 (2013); https://doi.org/10.1021/ja408329q
61. T. Tang, W.J. Jiang, S. Niu, N. Liu, H. Luo, Y.Y. Chen, S.F. Jin, F. Gao, L.J. Wan and J.S. Hu, *J. Am. Chem. Soc.*, **139**, 8320 (2017); https://doi.org/10.1021/jacs.7b03507
62. J. Kibsgaard and T.F. Jaramillo, *Angew. Chem. Int. Ed.*, **53**, 14433 (2014); https://doi.org/10.1002/anie.201408222
63. Y.-R. Liu, X. Shang, W.-K. Gao, B. Dong, J.-Q. Chi, X. Li, K.-L. Yan, Y.-M. Chai, Y.-Q. Liu and C.-G. Liu, *Appl. Surf. Sci.*, **412**, 138 (2017); https://doi.org/10.1016/j.apsusc.2017.03.245